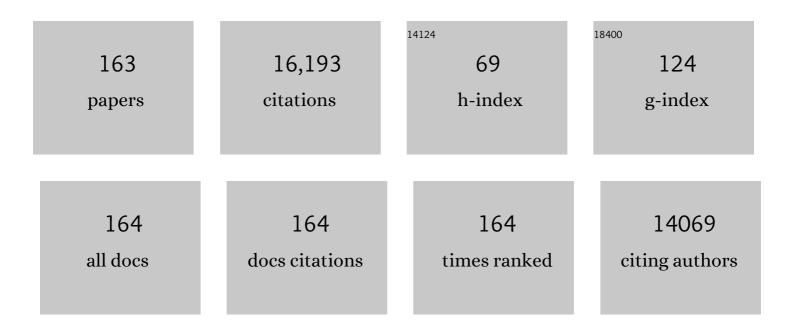
List of Publications by Year in descending order

Source: https://exaly.com/author-pdf/802658/publications.pdf Version: 2024-02-01



HUO-CEN YU

#	Article	IF	CITATIONS
1	CdIn ₂ S _{4â€} <i>_x</i> Se <i>_x</i> Solidâ€Solution Nanocrystal Photocatalyst: Oneâ€Step Hydrothermal Synthesis, Controllable Band Structure, and Improved H ₂ â€Evolution Activity. Advanced Sustainable Systems, 2023, 7, .	2.7	10
2	Cyano group-enriched crystalline graphitic carbon nitride photocatalyst: Ethyl acetate-induced improved ordered structure and efficient hydrogen-evolution activity. Journal of Colloid and Interface Science, 2022, 608, 1268-1277.	5.0	29
3	Inorganic Metalâ€Oxide Photocatalyst for H ₂ O ₂ Production. Small, 2022, 18, e2104561.	5.2	152
4	Simultaneously Optimizing the Number and Efficiency of Active Se Sites in Seâ€Rich <i>a</i> â€MoSe _{<i>x</i>} Nanodot Cocatalysts for Efficient Photocatalytic H ₂ Evolution. Solar Rrl, 2022, 6, .	3.1	14
5	Optimizing Atomic Hydrogen Desorption of Sulfurâ€Rich NiS ₁₊ <i>_x</i> Cocatalyst for Boosting Photocatalytic H ₂ Evolution. Advanced Materials, 2022, 34, e2108475.	11.1	156
6	Unsaturated selenium-enriched MoSe2+ amorphous nanoclusters: One-step photoinduced co-reduction route and its boosted photocatalytic H2-evolution activity for TiO2. Applied Catalysis B: Environmental, 2022, 305, 121053.	10.8	53
7	Emerging Sâ€ S cheme Photocatalyst. Advanced Materials, 2022, 34, e2107668.	11.1	717
8	<i>In situ</i> sulfuration synthesis of heterostructure MoS ₂ –Mo ₂ C@C for boosting the photocatalytic H ₂ production activity of TiO ₂ . Journal of Materials Chemistry C, 2022, 10, 3121-3128.	2.7	25
9	Palladium-copper nanodot as novel H2-evolution cocatalyst: Optimizing interfacial hydrogen desorption for highly efficient photocatalytic activity. Chinese Journal of Catalysis, 2022, 43, 215-225.	6.9	39
10	A one-step solvothermal synthesis of the topological insulator Bi ₂ Te ₃ nanorod-modified TiO ₂ photocatalyst for enhanced H ₂ -evolution activity. Journal of Materials Chemistry C, 2022, 10, 6402-6410.	2.7	15
11	Increasing unsaturated Se number and facilitating atomic hydrogen adsorption of WSe _{2+<i>x</i>} nanodots for improving photocatalytic H ₂ production of TiO ₂ . Journal of Materials Chemistry A, 2022, 10, 7989-7998.	5.2	30
12	Novel core-shell Ag@AgSe nanoparticle co-catalyst: In situ surface selenization for efficient photocatalytic H2 production of TiO2. Chinese Journal of Catalysis, 2022, 43, 1074-1083.	6.9	30
13	Phosphorus-enriched platinum diphosphide nanodots as a highly efficient cocatalyst for photocatalytic H2 evolution of CdS. Chemical Engineering Journal, 2022, 439, 135758.	6.6	79
14	Photoinduced self-stability mechanism of CdS photocatalyst: The dependence of photocorrosion and H2-evolution performance. Journal of Materials Science and Technology, 2022, 121, 19-27.	5.6	78
15	Mass-transfer control for selective deposition of well-dispersed AuPd cocatalysts to boost photocatalytic H2O2 production of BiVO4. Chemical Engineering Journal, 2022, 443, 136429.	6.6	26
16	Electron-enriched regulation of sulfur-active site for accelerating atomic hydrogen desorption of S-rich MoWS2+ cocatalyst toward efficient photocatalytic H2 evolution of TiO2. Chemical Engineering Journal, 2022, 449, 137803.	6.6	17
17	Dispersible CdS1â^'Se solid-solution nanocrystal photocatalysts: Photoinduced self-transformation synthesis and enhanced hydrogen-evolution activity. Journal of Colloid and Interface Science, 2022, 627, 320-331.	5.0	5
18	Sulfur-mediated photodeposition synthesis of NiS cocatalyst for boosting H2-evolution performance of g-C3N4 photocatalyst. Chinese Journal of Catalysis, 2021, 42, 37-45.	6.9	141

#	Article	IF	CITATIONS
19	Ultra-small molybdenum sulfide nanodot-coupled graphitic carbon nitride nanosheets: Trifunctional ammonium tetrathiomolybdate-assisted synthesis and high photocatalytic hydrogen evolution. Journal of Colloid and Interface Science, 2021, 586, 719-729.	5.0	30
20	Selenium-enriched amorphous NiSe1+ nanoclusters as a highly efficient cocatalyst for photocatalytic H2 evolution. Chemical Engineering Journal, 2021, 408, 127230.	6.6	60
21	Photoinduced synthesis of ultrasmall amorphous NiWSx nanodots for boosting photocatalytic H2-evolution activity of TiO2. Journal of Physics and Chemistry of Solids, 2021, 149, 109796.	1.9	10
22	Covalently functionalized graphene by thiourea for enhancing H2-evolution performance of TiO2 photocatalyst. Ceramics International, 2021, 47, 654-661.	2.3	23
23	Hetero-phase MoC-Mo2C nanoparticles for enhanced photocatalytic H2-production activity of TiO2. Nano Research, 2021, 14, 1095-1102.	5.8	57
24	Simultaneous realization of sulfur-rich surface and amorphous nanocluster of NiS1+ cocatalyst for efficient photocatalytic H2 evolution. Applied Catalysis B: Environmental, 2021, 280, 119455.	10.8	105
25	Oneâ€Step Realization of Crystallization and Cyanoâ€Group Generation for gâ€C ₃ N ₄ Photocatalysts with Improved H ₂ Production. Solar Rrl, 2021, 5, 2000372.	3.1	91
26	Hydroxyl-enriched highly crystalline TiO ₂ suspensible photocatalyst: facile synthesis and superior H ₂ -generation activity. Chemical Communications, 2021, 57, 2025-2028.	2.2	15
27	Highly dispersed MoS _x nanodot-modified TiO ₂ photocatalysts: vitamin C-mediated synthesis and improved H ₂ evolution activity. Journal of Materials Chemistry C, 2021, 9, 3239-3246.	2.7	27
28	One-step calcination synthesis of WC–Mo ₂ C heterojunction nanoparticles as novel H ₂ -production cocatalysts for enhanced photocatalytic activity of TiO ₂ . Catalysis Science and Technology, 2021, 11, 7307-7315.	2.1	19
29	Design, Fabrication, and Mechanism of Nitrogenâ€Doped Grapheneâ€Based Photocatalyst. Advanced Materials, 2021, 33, e2003521.	11.1	324
30	In Situ Synthesis of Mo ₂ C Nanoparticles on Graphene Nanosheets for Enhanced Photocatalytic H ₂ -Production Activity of TiO ₂ . ACS Sustainable Chemistry and Engineering, 2021, 9, 3828-3837.	3.2	56
31	Simultaneous realization of direct photodeposition and high H2-production activity of amorphous cobalt sulfide nanodot-modified rGO/TiO2 photocatalyst. Rare Metals, 2021, 40, 3125-3134.	3.6	49
32	Selenium-Rich Configuration and Amorphization for Synergistically Maximizing the Active-Center Amount of CoSe _{1+<i>x</i>} Nanodots toward Efficient Photocatalytic H ₂ Evolution. ACS Sustainable Chemistry and Engineering, 2021, 9, 8653-8662.	3.2	22
33	Amino group-rich porous g-C3N4 nanosheet photocatalyst: Facile oxalic acid-induced synthesis and improved H2-evolution activity. Ceramics International, 2021, 47, 18295-18303.	2.3	34
34	Synergism of tellurium-rich structure and amorphization of NiTe1+ nanodots for efficient photocatalytic H2-evolution of TiO2. Applied Catalysis B: Environmental, 2021, 290, 120057.	10.8	42
35	Fewâ€Layered Mo _{<i>x</i>} W _{1â^'<i>x</i>} S ₂ â€Modified CdS Photocatalyst: Oneâ€Step Synthesis with Bifunctional Precursors and Improved H ₂ â€Evolution Activity. Solar Rrl, 2021, 5, 2100387.	3.1	19
36	Novel amorphous NiCuS H2-evolution cocatalyst: Optimizing surface hydrogen desorption for efficient photocatalytic activity. Chemical Engineering Journal, 2021, 419, 129652.	6.6	76

#	Article	IF	CITATIONS
37	Selective modification of ultra-thin g-C3N4 nanosheets on the (110) facet of Au/BiVO4 for boosting photocatalytic H2O2 production. Applied Catalysis B: Environmental, 2021, 297, 120414.	10.8	63
38	EDTA-assisted synthesis of amorphous BiS nanodots for improving photocatalytic hydrogen-evolution rate of TiO2. Journal of Alloys and Compounds, 2021, 887, 161425.	2.8	21
39	Photocatalytic H ₂ Evolution Coupled with Furfuralcohol Oxidation over Ptâ€Modified ZnCdS Solid Solution. Small Methods, 2021, 5, e2100979.	4.6	79
40	BiVO ₄ Microparticles Decorated with Cu@Au Core-Shell Nanostructures for Photocatalytic H ₂ O ₂ Production. ACS Applied Nano Materials, 2021, 4, 13158-13166.	2.4	21
41	Core-shell Ag@Ni cocatalyst on the TiO2 photocatalyst: One-step photoinduced deposition and its improved H2-evolution activity. Applied Catalysis B: Environmental, 2020, 260, 118190.	10.8	171
42	Boosting antiphotocorrosion and hydrogen-production activity of cadmium sulfide by cobalt lactate complex. Applied Surface Science, 2020, 512, 144786.	3.1	16
43	Homojunction CdS Photocatalysts with a Massive S ^{2–} -Adsorbed Surface Phase: One-Step Facile Synthesis and High H ₂ -Evolution Performance. ACS Sustainable Chemistry and Engineering, 2020, 8, 543-551.	3.2	58
44	Edge-selectively amidated graphene for boosting H2-evolution activity of TiO2 photocatalyst. Applied Catalysis B: Environmental, 2020, 264, 118504.	10.8	61
45	Triethanolamine-assisted photodeposition of non-crystalline Cu _x P nanodots for boosting photocatalytic H ₂ evolution of TiO ₂ . Journal of Materials Chemistry C, 2020, 8, 15816-15822.	2.7	31
46	Colloidal CdS and CdZnS nanocrystal photocatalysts with massive S ^{2â^'} -adsorption: one-step facile synthesis and highly efficient H ₂ -evolution performance. Chemical Communications, 2020, 56, 9316-9319.	2.2	47
47	Boosting the H2-evolution performance of TiO2/Au photocatalyst by the facile addition of thiourea molecules. Applied Surface Science, 2020, 532, 147420.	3.1	21
48	Highly efficient S2â^'-adsorbed MoS -modified TiO2 photocatalysts: A general grafting strategy and boosted interfacial charge transfer. Journal of Materials Science and Technology, 2020, 56, 122-132.	5.6	58
49	Plasmonic Z-scheme Pt-Au/BiVO4 photocatalyst: Synergistic effect of crystal-facet engineering and selective loading of Pt-Au cocatalyst for improved photocatalytic performance. Journal of Colloid and Interface Science, 2020, 570, 232-241.	5.0	51
50	Carbon-coated cubic-phase molybdenum carbide nanoparticle for enhanced photocatalytic H2-evolution performance of TiO2. Journal of Energy Chemistry, 2020, 51, 253-261.	7.1	44
51	Porous crystalline g-C3N4: Bifunctional NaHCO3 template-mediated synthesis and improved photocatalytic H2-evolution rate. Applied Catalysis B: Environmental, 2020, 271, 118899.	10.8	134
52	Triethanolamine-mediated photodeposition formation of amorphous Ni-P alloy for improved H2-evolution activity of g-C3N4. Science China Materials, 2020, 63, 2215-2227.	3.5	53
53	Carboxyl-Functionalized Graphene for Highly Efficient H ₂ -Evolution Activity of TiO ₂ Photocatalyst. Wuli Huaxue Xuebao/ Acta Physico - Chimica Sinica, 2020, .	2.2	23
54	Self-templated formation of AgCl/TiO2 hollow octahedra for improved visible-light photocatalytic activity. Applied Surface Science, 2019, 494, 740-748.	3.1	17

#	Article	IF	CITATIONS
55	Silver-melamine nanowire-assisted synthesis of net-like AgCl-Ag/g-C3N4 for highly efficient photocatalytic degradation ability. Journal of Alloys and Compounds, 2019, 806, 263-271.	2.8	28
56	NH4Cl-induced low-temperature formation of nitrogen-rich g-C3N4 nanosheets with improved photocatalytic hydrogen evolution. Carbon, 2019, 153, 757-766.	5.4	132
57	Soluble g-C3N4 nanosheets: Facile synthesis and application in photocatalytic hydrogen evolution. Applied Catalysis B: Environmental, 2019, 247, 70-77.	10.8	217
58	Improved H2-generation performance of Pt/CdS photocatalyst by a dual-function TiO2 mediator for effective electron transfer and hole blocking. Ceramics International, 2019, 45, 9807-9813.	2.3	53
59	Ethyl acetate-induced formation of amorphous MoSx nanoclusters for improved H2-evolution activity of TiO2 photocatalyst. Chemical Engineering Journal, 2019, 375, 121934.	6.6	81
60	Efficient etching of oxygen-incorporated molybdenum disulfide nanosheet arrays for excellent electrocatalytic hydrogen evolution. Applied Surface Science, 2019, 491, 245-255.	3.1	22
61	Simultaneous Realization of Direct Photoinduced Deposition and Improved H ₂ -Evolution Performance of Sn-Nanoparticle-Modified TiO ₂ Photocatalyst. ACS Sustainable Chemistry and Engineering, 2019, 7, 10084-10094.	3.2	81
62	High-yield lactic acid-mediated route for a g-C ₃ N ₄ nanosheet photocatalyst with enhanced H ₂ -evolution performance. Nanoscale, 2019, 11, 9608-9616.	2.8	107
63	Ni nanoparticles as electron-transfer mediators and NiS as interfacial active sites for coordinative enhancement of H2-evolution performance of TiO2. Chinese Journal of Catalysis, 2019, 40, 343-351.	6.9	109
64	Highly efficient BiVO ₄ single-crystal photocatalyst with selective Ag ₂ O-Ag modification: orientation transport, rapid interfacial transfer and catalytic reaction. Dalton Transactions, 2018, 47, 6370-6377.	1.6	56
65	Facile synthesis and improved photocatalytic performance of Ag-AgCl photocatalyst by loading basic zinc carbonate. Journal of Alloys and Compounds, 2018, 752, 238-246.	2.8	24
66	Suspensible Cubic-Phase CdS Nanocrystal Photocatalyst: Facile Synthesis and Highly Efficient H ₂ -Evolution Performance in a Sulfur-Rich System. ACS Sustainable Chemistry and Engineering, 2018, 6, 5513-5523.	3.2	110
67	In situ photodeposition of amorphous CoS x on the TiO 2 towards hydrogen evolution. Applied Surface Science, 2018, 430, 448-456.	3.1	70
68	Synergistic effect of electron-transfer mediator and interfacial catalytic active-site for the enhanced H2-evolution performance: A case study of CdS-Au photocatalyst. Applied Catalysis B: Environmental, 2018, 220, 561-569.	10.8	160
69	Promoting the interfacial H2-evolution reaction of metallic Ag by Ag2S cocatalyst: A case study of TiO2/Ag-Ag2S photocatalyst. Applied Catalysis B: Environmental, 2018, 225, 415-423.	10.8	164
70	Highly efficient dual cocatalyst-modified TiO 2 photocatalyst: RGO as electron-transfer mediator and MoS x as H 2 -evolution active site. Applied Surface Science, 2018, 430, 176-183.	3.1	61
71	In situ one-step hydrothermal synthesis of oxygen-containing groups-modified g-C3N4 for the improved photocatalytic H2-evolution performance. Applied Surface Science, 2018, 427, 645-653.	3.1	189
72	One-step facile synthesis and high H ₂ -evolution activity of suspensible Cd _x Zn _{1â^*x} S nanocrystal photocatalysts in a S ^{2â^*} /SO ₃ ^{2â^*} system. Nanoscale, 2018, 10, 19418-19426.	2.8	64

#	Article	IF	CITATIONS
73	In-situ synthesis of amorphous H2TiO3-modified TiO2 and its improved photocatalytic H2-evolution performance. Journal of Colloid and Interface Science, 2018, 532, 272-279.	5.0	24
74	Direct Photoinduced Synthesis of Amorphous CoMoS _{<i>x</i>} Cocatalyst and Its Improved Photocatalytic H ₂ -Evolution Activity of CdS. ACS Sustainable Chemistry and Engineering, 2018, 6, 12436-12445.	3.2	86
75	Direct photoinduced synthesis and high H2-evolution performance of Bi-modified TiO2 photocatalyst in a Bi(III)-EG complex system. Applied Surface Science, 2018, 462, 623-632.	3.1	43
76	A facile hydrothermal synthesis of carbon dots modified g-C ₃ N ₄ for enhanced photocatalytic H ₂ -evolution performance. Dalton Transactions, 2017, 46, 6417-6424.	1.6	142
77	Ag-Modified BiOCl Single-Crystal Nanosheets: Dependence of Photocatalytic Performance on the Region-Selective Deposition of Ag Nanoparticles. Journal of Physical Chemistry C, 2017, 121, 13191-13201.	1.5	106
78	Synergistic effect of CoPi-hole and Cu(<scp>ii</scp>)-electron cocatalysts for enhanced photocatalytic activity and photoinduced stability of Ag ₃ PO ₄ . Physical Chemistry Chemical Physics, 2017, 19, 10309-10316.	1.3	33
79	Facile synthesis and enhanced photocatalytic H 2 -evolution performance of NiS 2 -modified g-C 3 N 4 photocatalysts. Chinese Journal of Catalysis, 2017, 38, 296-304.	6.9	153
80	lce–Water Quenching Induced Ti ³⁺ Self-doped TiO ₂ with Surface Lattice Distortion and the Increased Photocatalytic Activity. Journal of Physical Chemistry C, 2017, 121, 19836-19848.	1.5	69
81	Co-modification of amorphous-Ti(IV) hole cocatalyst and Ni(OH) 2 electron cocatalyst for enhanced photocatalytic H 2 -production performance of TiO 2. Applied Surface Science, 2017, 391, 259-266.	3.1	97
82	Selective adsorption of thiocyanate anions on Ag-modified g-C3N4 for enhanced photocatalytic hydrogen evolution. Chinese Journal of Catalysis, 2017, 38, 1990-1998.	6.9	120
83	Amorphous Ti(<scp>iv</scp>)-modified Bi ₂ WO ₆ with enhanced photocatalytic performance. RSC Advances, 2016, 6, 65902-65910.	1.7	22
84	Amorphous molybdenum sulfide as highly efficient electron-cocatalyst for enhanced photocatalytic H2 evolution. Applied Catalysis B: Environmental, 2016, 193, 217-225.	10.8	223
85	Highly efficient TiO ₂ single-crystal photocatalyst with spatially separated Ag and F ^{â^'} bi-cocatalysts: orientation transfer of photogenerated charges and their rapid interfacial reaction. Journal of Materials Chemistry A, 2016, 4, 8682-8689.	5.2	148
86	Synchronous synthesis/modification of multifunctional hollow silica nanospheres through selective etching and application in catalysis. Colloids and Surfaces A: Physicochemical and Engineering Aspects, 2016, 509, 648-655.	2.3	4
87	In situ hydrothermal synthesis and enhanced photocatalytic H 2 -evolution performance of suspended rGO/g-C 3 N 4 photocatalysts. Journal of Molecular Catalysis A, 2016, 424, 369-376.	4.8	47
88	Phenylamine-Functionalized rGO/TiO ₂ Photocatalysts: Spatially Separated Adsorption Sites and Tunable Photocatalytic Selectivity. ACS Applied Materials & Interfaces, 2016, 8, 29470-29477.	4.0	122
89	Enhanced photocatalytic activity and photoinduced stability of Ag-based photocatalysts: The synergistic action of amorphous-Ti(IV) and Fe(III) cocatalysts. Applied Catalysis B: Environmental, 2016, 187, 163-170.	10.8	109
90	Visible-Light-Sensitive Photocatalysts: Nanocluster-Grafted Titanium Dioxide for Indoor Environmental Remediation. Journal of Physical Chemistry Letters, 2016, 7, 75-84.	2.1	138

#	Article	IF	CITATIONS
91	Hierarchically macro–mesoporous TiO2 film via self-assembled strategy for enhanced efficiency of dye sensitized solar cells. Materials Research Bulletin, 2016, 74, 380-386.	2.7	21
92	Enhanced Photoinduced-Stability and Photocatalytic Activity of CdS by Dual Amorphous Cocatalysts: Synergistic Effect of Ti(IV)-Hole Cocatalyst and Ni(II)-Electron Cocatalyst. Journal of Physical Chemistry C, 2016, 120, 3722-3730.	1.5	195
93	A novel functional group difference-based selective etching strategy for the synthesis of hollow organic silica nanospheres. RSC Advances, 2016, 6, 26914-26920.	1.7	3
94	Selective basic etching of bifunctional core–shell composite particles for the fabrication of organic functionalized hollow mesoporous silica nanospheres. New Journal of Chemistry, 2016, 40, 825-831.	1.4	11
95	The synergistic effect of graphitic N and pyrrolic N for the enhanced photocatalytic performance of nitrogen-doped graphene/TiO2 nanocomposites. Applied Catalysis B: Environmental, 2016, 181, 810-817.	10.8	287
96	Synergistic Effect of Dual Electron-Cocatalysts for Enhanced Photocatalytic Activity: rGO as Electron-Transfer Mediator and Fe(III) as Oxygen-Reduction Active Site. Scientific Reports, 2015, 5, 13083.	1.6	43
97	Co-modification of Fâ^' and Fe(III) ions as a facile strategy towards effective separation of photogenerated electrons and holes. Applied Surface Science, 2015, 351, 66-73.	3.1	26
98	Facile template-induced synthesis of Ag-modified TiO2 hollow octahedra with high photocatalytic activity. Chinese Journal of Catalysis, 2015, 36, 1211-2218.	6.9	46
99	Graphene oxide nanosheets as an effective template for the synthesis of porous TiO2 film in dye-sensitized solar cells. Applied Surface Science, 2015, 358, 175-180.	3.1	35
100	Facile synthesis of porous Bi ₂ WO ₆ nanosheets with high photocatalytic performance. Dalton Transactions, 2015, 44, 14532-14539.	1.6	50
101	In situ self-transformation synthesis of g-C3N4-modified CdS heterostructure with enhanced photocatalytic activity. Applied Surface Science, 2015, 358, 385-392.	3.1	156
102	Facile preparation of photocatalytic exposed aggregate concrete with highly efficient and stable catalytic performance. Chemical Engineering Journal, 2015, 264, 577-586.	6.6	37
103	Agl-BiOI Spherical Solid Solutions with Enhanced Visible-Light Photocatalytic Performances. Current Nanoscience, 2015, 11, 453-461.	0.7	4
104	Cu ₂ O-rGO-CuO Composite: An Effective Z-scheme Visible-Light Photocatalyst. Current Nanoscience, 2015, 11, 462-469.	0.7	11
105	Nanosized Photocatalytic Materials 2013. Journal of Nanomaterials, 2014, 2014, 1-2.	1.5	0
106	Greatly enhanced photocatalytic activity of TiO2â^'xNx by a simple surface modification of Fe(III) cocatalyst. Journal of Molecular Catalysis A, 2014, 391, 92-98.	4.8	34
107	Enhanced photoinduced stability and photocatalytic activity of AgBr photocatalyst by surface modification of Fe(III) cocatalyst. Applied Catalysis B: Environmental, 2014, 144, 75-82.	10.8	130
108	Joint optimal sensing time and power allocation for multi-channel cognitive radio networks considering sensing-channel selection. Science China Information Sciences, 2014, 57, 1-8.	2.7	8

#	Article	IF	CITATIONS
109	Cocatalyst modification and nanonization of Ag/AgCl photocatalyst with enhanced photocatalytic performance. Journal of Molecular Catalysis A, 2014, 381, 114-119.	4.8	38
110	Enhanced photocatalytic performance of Ag3PO4 by simutaneous loading of Ag nanoparticles and Fe(III) cocatalyst. Applied Catalysis B: Environmental, 2014, 160-161, 658-665.	10.8	110
111	Improved high-rate performance and cycling stability of 1D LiFePO4 nanorods by a facile annealing process. Journal Wuhan University of Technology, Materials Science Edition, 2014, 29, 656-659.	0.4	2
112	Cu(II) as a General Cocatalyst for Improved Visible-Light Photocatalytic Performance of Photosensitive Ag-Based Compounds. Journal of Physical Chemistry C, 2014, 118, 8891-8898.	1.5	65
113	Dependence of metallic Ag on the photocatalytic activity and photoinduced stability of Ag/AgCl photocatalyst. Applied Surface Science, 2014, 319, 324-331.	3.1	47
114	Facile synthesis and enhanced visible-light photocatalytic activity of Ag2S nanocrystal-sensitized Ag8W4O16 nanorods. Journal of Colloid and Interface Science, 2014, 422, 30-37.	5.0	35
115	Dye-Sensitization-Induced Visible-Light Reduction of Graphene Oxide for the Enhanced TiO ₂ Photocatalytic Performance. ACS Applied Materials & Interfaces, 2013, 5, 2924-2929.	4.0	139
116	Facile Fabrication and Enhanced Photocatalytic Performance of Ag/AgCl/rGO Heterostructure Photocatalyst. ACS Applied Materials & Interfaces, 2013, 5, 2161-2168.	4.0	164
117	One-step synthesis of easy-recycling TiO2-rGO nanocomposite photocatalysts with enhanced photocatalytic activity. Applied Catalysis B: Environmental, 2013, 132-133, 452-459.	10.8	396
118	Hierarchically porous metastable β-Ag ₂ WO ₄ hollow nanospheres: controlled synthesis and high photocatalytic activity. Nanotechnology, 2013, 24, 165602.	1.3	72
119	Environmental Photocatalysis 2013. International Journal of Photoenergy, 2013, 2013, 1-3.	1.4	4
120	Enhancement of Visible-Light Photocatalytic Activity of Mesoporous Au-TiO ₂ Nanocomposites by Surface Plasmon Resonance. International Journal of Photoenergy, 2012, 2012, 1-10.	1.4	28
121	Facile Preparation and Photoinduced Superhydrophilicity of Highly Ordered Sodium-Free Titanate Nanotube Films by Electrophoretic Deposition. International Journal of Photoenergy, 2012, 2012, 1-6.	1.4	4
122	One-Pot Template-Free Hydrothermal Synthesis of Monoclinic Hollow Microspheres and Their Enhanced Visible-Light Photocatalytic Activity. International Journal of Photoenergy, 2012, 2012, 1-10.	1.4	17
123	Environmental Photocatalysis. International Journal of Photoenergy, 2012, 2012, 1-4.	1.4	5
124	UV- and Visible-Light Photocatalytic Activity of Simultaneously Deposited and Doped Ag/Ag(I)-TiO ₂ Photocatalyst. Journal of Physical Chemistry C, 2012, 116, 17721-17728.	1.5	233
125	Synthesis, Characterization, Properties, and Applications of Nanosized Photocatalytic Materials. Journal of Nanomaterials, 2012, 2012, 1-3.	1.5	12
126	The dependence of photocatalytic activity and photoinduced self-stability of photosensitive AgI nanoparticles. Dalton Transactions, 2012, 41, 10405.	1.6	87

#	Article	IF	CITATIONS
127	Self-assembled synthesis of porous TiO2 film on the electrophoretic-deposited titanate nanoribbon film. Journal Wuhan University of Technology, Materials Science Edition, 2012, 27, 203-206.	0.4	0
128	Selective-adsorption removal of methyl orange(MO) by CTAB-assisted AgBr powder. Journal Wuhan University of Technology, Materials Science Edition, 2012, 27, 675-678.	0.4	3
129	Enhanced visible-light photocatalytic activity of Bi2WO6 nanoparticles by Ag2O cocatalyst. Applied Catalysis B: Environmental, 2012, 111-112, 326-333.	10.8	259
130	One-pot pyridine-assisted synthesis of visible-light-driven photocatalyst Ag/Ag3PO4. Applied Catalysis B: Environmental, 2012, 115-116, 245-252.	10.8	218
131	H ₂ WO ₄ ·H ₂ O/Ag/AgCl Composite Nanoplates: A Plasmonic Z-Scheme Visible-Light Photocatalyst. Journal of Physical Chemistry C, 2011, 115, 14648-14655.	1.5	255
132	Ag ₂ O as a New Visibleâ€Light Photocatalyst: Selfâ€Stability and High Photocatalytic Activity. Chemistry - A European Journal, 2011, 17, 7777-7780.	1.7	423
133	In situ anion-exchange synthesis and photocatalytic activity of Ag8W4O16/AgCl-nanoparticle core–shell nanorods. Journal of Molecular Catalysis A, 2011, 334, 52-59.	4.8	80
134	Low-temperature hydrothermal synthesis of highly photoactive mesoporous spherical TiO2 nanocrystalline. Journal of Physics and Chemistry of Solids, 2010, 71, 507-510.	1.9	20
135	Fabrication of Ru(bpy)32+-titanate nanotube nanocomposite and its application as sensitive solid-state electrochemiluminescence sensor material. Journal of Physics and Chemistry of Solids, 2010, 71, 527-529.	1.9	9
136	Conduction Band Energy Level Control of Titanium Dioxide: Toward an Efficient Visible-Light-Sensitive Photocatalyst. Journal of the American Chemical Society, 2010, 132, 6898-6899.	6.6	282
137	Visible-Light-Driven Cu(II)â [~] (Sr _{1â[~] <i>y</i>} Na _{<i>y</i>})(Ti _{1â[~] <i>x</i>} Mo _{<i>x</i>Photocatalysts Based on Conduction Band Control and Surface Ion Modification. Journal of the American Chemical Society, 2010, 132, 15259-15267.}	>)Q	3 <u sub>
138	An Efficient Visible-Light-Sensitive Fe(III)-Grafted TiO ₂ Photocatalyst. Journal of Physical Chemistry C, 2010, 114, 16481-16487.	1.5	344
139	Effects of urea on the microstructure and photocatalytic activity of bimodal mesoporous titania microspheres. Journal of Molecular Catalysis A, 2009, 313, 107-113.	4.8	28
140	Spontaneous Formation of a Tungsten Trioxide Sphereâ€inâ€5hell Superstructure by Chemically Induced Selfâ€Transformation. Small, 2008, 4, 87-91.	5.2	176
141	A One-Pot Approach to Hierarchically Nanoporous Titania Hollow Microspheres with High Photocatalytic Activity. Crystal Growth and Design, 2008, 8, 930-934.	1.4	244
142	Novel preparation and photocatalytic activity of one-dimensional TiO2hollow structures. Nanotechnology, 2007, 18, 065604.	1.3	56
143	Photocatalytic activity of the calcined H-titanate nanowires for photocatalytic oxidation of acetone in air. Chemosphere, 2007, 66, 2050-2057.	4.2	52
144	Synthesis, characterization and photocatalytic activity of mesoporous titania nanorod/titanate nanotube composites. Journal of Hazardous Materials, 2007, 147, 581-587.	6.5	107

#	Article	IF	CITATIONS
145	Microstructures and photoactivity of mesoporous anatase hollow microspheres fabricated by fluoride-mediated self-transformation. Journal of Catalysis, 2007, 249, 59-66.	3.1	359
146	Template-free Hydrothermal Synthesis of CuO/Cu ₂ O Composite Hollow Microspheres. Chemistry of Materials, 2007, 19, 4327-4334.	3.2	450
147	Facile preparation of Na-free anatase TiO2 film with highly photocatalytic activity on soda-lime glass. Catalysis Communications, 2006, 7, 1000-1004.	1.6	26
148	Photocatalytic activity of dispersed TiO2 particles deposited on glass fibers. Journal of Molecular Catalysis A, 2006, 246, 206-211.	4.8	83
149	Enhanced photocatalytic activity of TiO2 powder (P25) by hydrothermal treatment. Journal of Molecular Catalysis A, 2006, 253, 112-118.	4.8	254
150	Preparation and photocatalytic activity of mesoporous anatase TiO2 nanofibers by a hydrothermal method. Journal of Photochemistry and Photobiology A: Chemistry, 2006, 182, 121-127.	2.0	181
151	Effects of hydrothermal post-treatment on microstructures and morphology of titanate nanoribbons. Journal of Solid State Chemistry, 2006, 179, 349-354.	1.4	131
152	Fabrication, characterization and photocatalytic activity of preferentially oriented TiO2 films. Journal of Crystal Growth, 2006, 295, 60-68.	0.7	22
153	Effects of calcination temperature on the microstructures and photocatalytic activity of titanate nanotubes. Journal of Molecular Catalysis A, 2006, 249, 135-142.	4.8	352
154	Preparation, characterization and photocatalytic activity of in situ Fe-doped TiO2 thin films. Thin Solid Films, 2006, 496, 273-280.	0.8	154
155	Preparation, characterization and photocatalytic activity of novel TiO2 nanoparticle-coated titanate nanorods. Journal of Molecular Catalysis A, 2006, 253, 99-106.	4.8	33
156	Enhanced photoinduced super-hydrophilicity of the sol–gel-derived TiO2 thin films by Fe-doping. Materials Chemistry and Physics, 2006, 95, 193-196.	2.0	77
157	Facile synthesis and characterization of novel nanocomposites of titanate nanotubes and rutile nanocrystals. Materials Chemistry and Physics, 2006, 100, 507-512.	2.0	52
158	Signature of Intrinsic High-Temperature Ferromagnetism in Cobalt-Doped Zinc Oxide Nanocrystals. Advanced Materials, 2006, 18, 2476-2480.	11.1	178
159	Low-temperature fabrication and photocatalytic activity of clustered TiO2 particles formed on glass fibers. Journal of Crystal Growth, 2005, 280, 612-619.	0.7	25
160	Ultrasonic preparation of mesoporous titanium dioxide nanocrystalline photocatalysts and evaluation of photocatalytic activity. Journal of Molecular Catalysis A, 2005, 227, 75-80.	4.8	128
161	Preparation and photocatalytic activity of Fe-doped mesoporous titanium dioxide nanocrystalline photocatalysts. Materials Chemistry and Physics, 2005, 93, 159-163.	2.0	204
162	The Effect of Calcination Temperature on the Surface Microstructure and Photocatalytic Activity of TiO2 Thin Films Prepared by Liquid Phase Deposition. Journal of Physical Chemistry B, 2003, 107, 13871-13879.	1.2	1,113

#	Article	IF	CITATIONS
163	Effects of Substrates on the Composition and Microstructure of TiO ₂ Thin Films Prepared by the LPD Method. Key Engineering Materials, 0, 280-283, 795-800.	0.4	1